

High-Voltage Polymers for High-Power Supercapacitors

WP1359

Dr. Nicholas Prokopuk
Naval Air Warfare Center, Weapons Division
China Lake, CA

May 30, 2006

Version 1

REPORT DOCUMENTATION PAGEForm Approved
OMB No. 0704-0188

Public reporting burden for this collection of information is estimated to average 1 hour per response, including the time for reviewing instructions, searching existing data sources, gathering and maintaining the data needed, and completing and reviewing this collection of information. Send comments regarding this burden estimate or any other aspect of this collection of information, including suggestions for reducing this burden to Department of Defense, Washington Headquarters Services, Directorate for Information Operations and Reports (0704-0188), 1215 Jefferson Davis Highway, Suite 1204, Arlington, VA 22202-4302. Respondents should be aware that notwithstanding any other provision of law, no person shall be subject to any penalty for failing to comply with a collection of information if it does not display a currently valid OMB control number. **PLEASE DO NOT RETURN YOUR FORM TO THE ABOVE ADDRESS.**

1. REPORT DATE (DD-MM-YYYY) 30-05-2006		2. REPORT TYPE Final		3. DATES COVERED (From - To) 30-05-2005 - 30-05-2006	
4. TITLE AND SUBTITLE High-Voltage Polymers for High-Power Supercapacitors				5a. CONTRACT NUMBER	
				5b. GRANT NUMBER	
				5c. PROGRAM ELEMENT NUMBER	
6. AUTHOR(S) Nicholas Prokopuk				5d. PROJECT NUMBER WP 1359	
				5e. TASK NUMBER	
				5f. WORK UNIT NUMBER	
7. PERFORMING ORGANIZATION NAME(S) AND ADDRESS(ES) Chemistry and Division Naval Air Warfare Center 1900 N. Knox Rd. STOP 6303 China Lake, CA 93555				8. PERFORMING ORGANIZATION REPORT NUMBER	
9. SPONSORING / MONITORING AGENCY NAME(S) AND ADDRESS(ES)				10. SPONSOR/MONITOR'S ACRONYM(S) NAWC, NAWCWD	
				11. SPONSOR/MONITOR'S REPORT NUMBER(S)	
12. DISTRIBUTION / AVAILABILITY STATEMENT Approved for public release; distribution is unlimited					
13. SUPPLEMENTARY NOTES					
14. ABSTRACT New polymer supercapacitors were constructed from novel hybrid poly(triarylamines) with organic electrolytes. The new polymers contain benzyl or nitro functionalized aromatic side groups. In addition to the anilino segments, the polymer backbone contains either furanyl or thiophenyl linkages. These electronic and structural varieties provide polymers with a range of oxidation potentials. The nitro-furane derivative exhibits the highest oxidation potential and supercapacitors constructed with anodes of this polymer and organic electrolytes provide 20% more power and energy than the polythiophene derivatives studied previously. These results indicate that the supercapacitor performance can be significantly altered by varying pendent substituents and the polymer backbone					
15. SUBJECT TERMS Polymers, supercapacitors					
16. SECURITY CLASSIFICATION OF:			17. LIMITATION OF ABSTRACT UU	18. NUMBER OF PAGES 24	19a. NAME OF RESPONSIBLE PERSON Nicholas Prokopuk
a. REPORT U	b. ABSTRACT U	c. THIS PAGE U			19b. TELEPHONE NUMBER (include area code) (760) 939-6735

This report was prepared under contract to the Department of Defense Strategic Environmental Research and Development Program (SERDP). The publication of this report does not indicate endorsement by the Department of Defense, nor should the contents be construed as reflecting the official policy or position of the Department of Defense. Reference herein to any specific commercial product, process, or service by trade name, trademark, manufacturer, or otherwise, does not necessarily constitute or imply its endorsement, recommendation, or favoring by the Department of Defense.

Table of Contents

List of Abbreviations	iii
Acknowledgements	iv
Executive Summary	1
Objective	2
Background	3
Materials and Methods	6
Results and Accomplishments	11
Conclusions	19
References	20

Abbreviations

mA	milliamp
s	second
V	volt
mm	millimeter
mmol	millimole
[Bu ₄ N] ⁺	tetrabutylammonium
[Me ₄ N] ⁺	tetramethylammonium
h	hour
g	gram
mL	milliliter
NMR	nuclear magnetic resonance
v	volume
DFT	density function theory
HOMO	highest occupied molecular orbital
mV	millivolt

Acknowledgements

The work described in this report was performed by the Chemistry and Materials branch at the Naval Air Warfare Center, Weapons Division, China Lake, California. Dr. Nicholas Prokopuk led the effort with Dr. Michael Wright, Mr. Andrew Chafin, Dr. David Witker, Dr. Lawrence Baldwin, and Dr. Jeffrey R. Deschamps (NRL) collaborating. Dr. Wright synthesized the new monomers and Dr. Baldwin performed their NMR characterization. Dr. Witker and Dr. Prokopuk performed the electrochemical polymerization and supercapacitor characterization experiments. Mr. Chafin performed the DFT calculations and Dr. Deschamps performed the X-ray work. This research was supported wholly by the U.S. Department of Defense, through the Strategic Environmental Research and Development Program (SERDP).

Executive Summary

Power supplies for the electronic fuses considered in the next generation of medium caliber munitions (20 – 60 mm) are primarily lithium-based chemical batteries. Lithium batteries are most commonly constructed from metallic lithium as the anode, thionyl chloride as the electrolyte, and a transition metal oxide or chalcogenide as the cathode. All three components are environmentally unacceptable and alternatives currently being used, such as sulfuryl chloride electrolytes, are equally harmful. Specifically, lithium metal reacts violently with water, causing burns and releasing hydrogen, which can ignite. Thionyl chloride and sulfuryl chloride are extremely caustic and decompose to yield hydrogen chloride, sulfur dioxide, and chlorine gas. The cathode materials often contain toxic cobalt. Repeated discharging of munitions containing lithium batteries will lead to long-term environmental problems and expensive clean up cost.

Alternatives to the lithium batteries must fit within the physical constraints of the medium caliber munitions, approximately a cylinder of 18 mm in diameter and 12.5 mm in height, and still provide comparable power and energy outputs. For the energy and power requirements, a supply of 4 V with a current drain of 20 – 200 mA for up to 10 s is required. In addition, the new power supply must be able to operate under the conditions of an extremely high linear acceleration (100+ KG) and spin rates (1000 – 1800 revolutions per second). Storage life times of more than 20 years and low cost are also desired. Previously, under SERDP support we demonstrated an all-organic supercapacitor as an alternative to lithium batteries. In these devices, two supercapacitors in series provide the necessary energy and power requirements within the allotted volume. By using a series configuration, the required output voltage of the capacitors is lowered to 2 V. Small variations in the anode or cathode polymer or electrolyte were found to significantly affect the supercapacitor's performance.

Subsequently, our efforts focused on fabricating polymers with high oxidation potentials to increase the power output of the supercapacitors. Novel hybrid polymers that exhibit a tunable oxidation potential were synthesized based on a poly(thiophenylanilino) and poly(furanylanilino) framework. In these novel materials, the triarylammine functionality provides a redox site with an oxidation potential that can be tuned by varying the substituents on the aromatic rings. Monomers with thiophene and furan pendant groups were prepared and fully characterized. By electrochemically oxidizing the ammine functionalities, the thiophene and furan groups polymerize. Polymers with oxidation potentials spanning 0.6 V were possible with only a limited range of functional groups and a single substitution on each ring.

The discharge properties of supercapacitors constructed from the new hybrid polymer cathodes and polythiophene and poly(3-methylthiophene) were measured in combination with chemically innocuous electrolytes. *These new supercapacitors displayed energy capacities that are 20 % greater than those composed of the conventional polythiophene polymers.* These new materials should enable an all-organic supercapacitor with even greater energy and power densities.

Objective

The objective of this work is to synthesize new polymers that exhibit more positive oxidation potentials than conventional polythiophenes and demonstrate at the laboratory scale a supercapacitor composed of these conductive polymers as the electrodes. The new polymers must exhibit oxidation potentials in excess of 0.7 V vs Ag/Ag⁺. Furthermore, supercapacitors derived from these polymers must employ only environmentally benign electrolytes and fit within the spatial limitations set by the medium caliber munitions (a cylinder of 18 mm in diameter and 12.5 mm in height). Finally, the discharge properties of the capacitors must provide a minimum current of 20 mA at 2 V for a minimum of 10 s. These metrics are required for the potential application of these power sources in medium caliber munitions.

Background

As the most electropositive metal, lithium has been used extensively in constructing high-energy batteries.¹ The highly negative reduction potential inherent to lithium (-3.05 V) and lightweight make for superior anodes surpassing most other metals in terms of energy density. In order to obtain batteries capable of providing significant currents (>200 mA) with voltages in excess of 3.5 V, electrolytes such as thionyl chloride SOCl_2 or sulfuryl chloride SO_2Cl_2 have been employed.² The combination of lithium metal and SOCl_2 or SO_2Cl_2 makes for toxic, corrosive, flammable, and potentially explosive batteries. Yet, replacing just the lithium anode with a more benign material will eliminate the requirement for the caustic electrolytes. Thus, our approach will focus on developing energy sources derived from all-organic supercapacitor.

Supercapacitors have been used commercially for sometime as power supplies to augment chemical batteries. Rechargeable batteries discharge at relatively low rates and, thus, have limited power supplies, Figure 1. When spikes in power are needed, a capacitor can supplement the primary energy source. The most common redox capacitor electrodes are comprised of toxic metals or costly nanocomposites.³ Supercapacitors derived exclusively from low-cost organic polymers offer an inexpensive alternative. However, few studies have focused on applying these devices as a primary power source due to their relatively low energy densities, Figure 1. Since the energy required to power the electric fuses of medium caliber munitions are quite low and the power demands are needed for only a short duration, the polymer supercapacitors are promising candidates for this specific and narrow application.

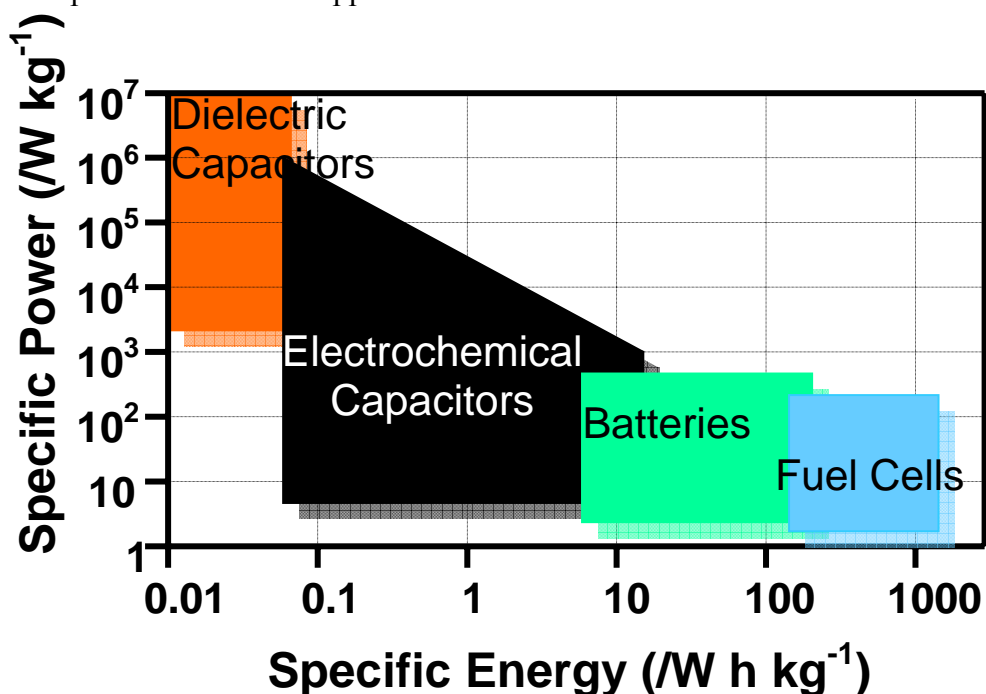


Figure 1. Ragone plot of common electrochemical devices.

The supercapacitors described in this proposal are especially convenient in that the polymer components are easily handled and processed and the devices are adaptable to existing methodologies for triggering including spin activation with out significant modifications.

Electroactive polymers such as polythiophene, polyacetylene, or polyaniline can be reduced, *n*-doped, or oxidized, *p*-doped.⁴ Reduction of the polymer raises the work function of the material and counter cations are incorporated into the polymer network during the process. Similarly, oxidizing an electroactive polymer lowers the work function of the material concomitant with anion intercalation. Electroactive polymers have been known for many years with applications in corrosion protection, sensors, LEDs, and non-linear optics.⁵ As electrodes in an organic supercapacitor, the potential difference between the two polymer films provides the energy to drive electric currents and voltages.⁶ Similarly, the energy difference between a lithium anode and a cobalt oxide cathode provide the potential energy in a lithium battery.

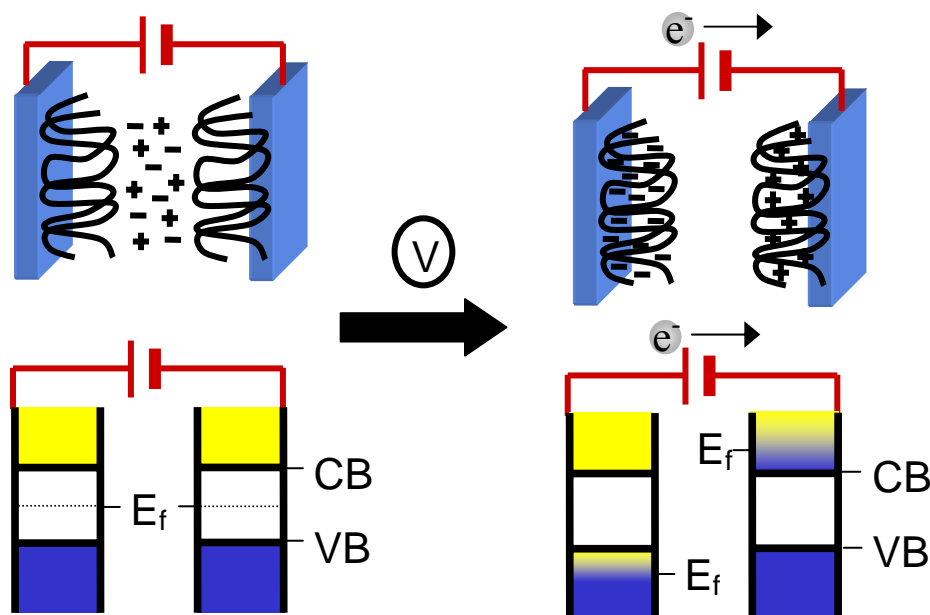


Figure 2. Prior to charging a polymer supercapacitor (top left), the polymer electrodes are neutral. After a potential is applied to charge the polymers (top right), charge compensating ions from the electrolyte migrate into the films. The energy diagram prior to charging has the Fermi level of the two polymer films equal (bottom left). After charging, the oxidized polymer has a lower Fermi energy and the reduced polymer has a higher Fermi level (bottom right).

As components of the supercapacitor, the *n*-doped and *p*-doped polymers must conduct both electrons and ions fast enough to deliver the desired currents. While the electronic conductivity of conjugated polymers has been studied quite extensively, very little is known about the ionic conductivity of these polymers.⁷⁻¹⁰ Slow ionic diffusion

within the polymers will restrict the electrical discharge rates and limit the performance of the capacitor. Ghosh and coworkers have made polymer blends of polythiophene, a good electronic conductor, and polyethyleneoxide, a good ionic conductor, to improve the electrical discharge rate.¹¹ Unfortunately, this improvement occurred at a cost of capacity. To date, the ionic conductivity of conjugated polymers remains poorly understood. As a result many electrochemical properties of these polymers are difficult or impossible to predict because they depend strongly on the electrolyte. For example, films of poly(3-methylthiophene) are oxidized at 0.54 V vs. SCE with LiPF₆ electrolytes versus 0.66 V with LiOSO₂CF₃.¹²

By contrast, ionic conductivity in electrically insulating polymers such as polyethyleneoxide is well understood and many polymer electrolytes have been synthesized which take advantage of recent advances in understanding ionic motion in polymer salt complexes.¹³ In many of these systems the segmental motion of the polymer backbone governs the mobility of the cations. To increase cationic motion, flexible polymers with low glass transition temperatures T_g are employed. For improved electrical conductivity in conjugated polymers, however, well-ordered and rigid structures are preferred.^{9,10} These competing requirements will have to be balanced in order to construct supercapacitors with fast ionic and electronic conductivity. Still in other polymer electrolytes, ionic motion is relatively independent of the polymer motion.¹⁴ In these systems the close proximity of low energy sites enables the cations to move through the material with only a minimal reorganization of the polymer.

Previously under SERDP support, we demonstrated a polythiophene supercapacitor that provides an output of 20 mA at 2 V for 10 s. While these metrics are suitable for many existing applications, higher output currents and densities will be needed for future applications. An increase in the power and energy density will allow for a more versatile power supply that will see greater deployment for a longer period of time. To address these needs, we have focused our efforts on designing and synthesizing polymer supercapacitors with enhanced voltages by using redox tunable materials.

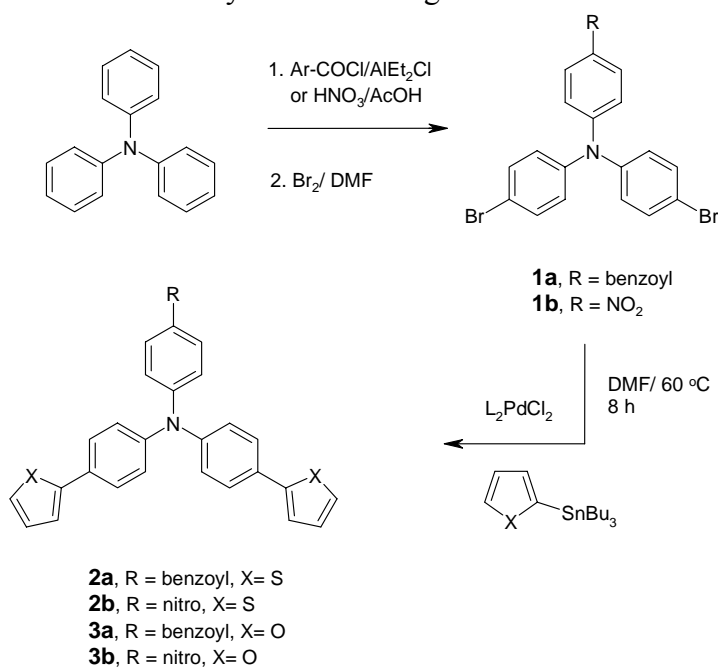
Materials and Methods

Materials

Acetonitrile (CH_3CN) was purchased from Aldrich and dried over CaH_2 under a nitrogen atmosphere and distilled prior to use. Methylthiophene (Aldrich) was distilled under vacuum prior to use. Bithiophene was used as received from Aldrich. Carbon paper was obtained from E-Tek, New Jersey. Tetrabutylammonium tetrafluoroborate $[\text{Bu}_4\text{N}]\text{BF}_4$ was prepared by adding aqueous solutions of the tetraalkylammonium salt of hydrogen sulfate and ammonium tetrafluoroborate. The resulting precipitate was isolated by filtration and recrystallized from acetonitrile and ether.

Monomer Synthesis

The new monomers were synthesized using the reaction scheme:



Scheme 1

The experimental details for each step are described below.

Friedel-Crafts benzoylation of triphenylamine. A chilled ($0\text{ }^\circ\text{C}$) dichloromethane (100 mL) solution containing triphenylamine (10.00 g, 40.8 mmol) and benzoyl chloride (41 mmol) was treated dropwise with diethylaluminum chloride (22 mL, ~40 mmol). After addition was complete the mixture was allowed to react at $0\text{ }^\circ\text{C}$ for 4 h with stirring. The mixture was carefully diluted with water (50 mL) and allowed to stir for 2 h. A saturated solution of sodium bicarbonate was added and the organic layer separated and then dried over MgSO_4 . The solvent was removed under reduce pressure

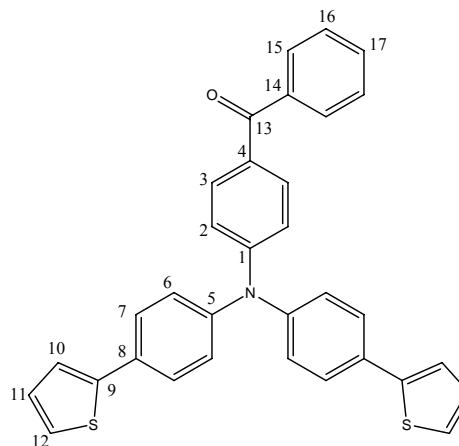
and crude product purified by column chromatography on silica gel using chloroform as the eluent.

General procedure for bromination. A chilled (0 °C) dichloromethane (100 mL) solution containing 4-(diphenylamino)benzophenone or 4-nitrotriphenylamine (~22.6 mmol) was treated dropwise with bromine (~50 mmol). After allowing the mixture to react at 0 °C for 2 h with stirring the mixture was diluted with saturated sodium bicarbonate (50 mL). The mixture was placed in a separatory funnel and the organic layer isolated and washed with water (100 mL), brine (50 mL), and then dried over MgSO₄. The solvent was removed under reduced pressure and the crude product was recrystallized from ethanol to afford analytically pure **1b**. In a similar manner compound **1a** was prepared using a dilute solution of nitric acid in acetic acid for deliverance of the electrophile (i.e. NO₂).

General procedure for the Stille cross-coupling of N,N'-bis(4-bromophenyl)-N''-(4-X-phenyl)amine (X= benzoyl, nitro) with 2-(tributylstannyl)thiophene (to afford 2a and 2b respectively) and 2-tributylstannylfuran (to afford 3a and 3b respectively). A Schlenk flask was charged with the appropriate dibromotriarylamine (10 mmol), organostannane reagent (20 mmol), (PPh₃)₂PdCl₂ (0.5 mmol), and DMF (25 mL). The mixture was heated at 50 °C for 24 h with stirring and then diluted with chloroform and washed with water (5 x 100 mL). The solvent was removed under reduced pressure and crude product was subjected to chromatography on silica gel (chloroform/hexanes, 8/2, v/v). The major band was collected and the solvents removed under reduced pressure the solid was recrystallized by diffusing pentane into a chloroform or acetone solution of the product. Solvent co-crystallization occurs for both acetone and chloroform.

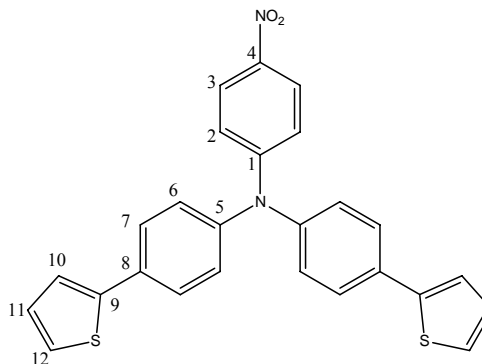
Spectroscopic data for **2a** (Figure 3): ¹H NMR (400 MHz, CDCl₃): 7.80 (d, *J*= 7.4 Hz, H15, 2H), 7.75 (d, *J*= 8.8 Hz, H3, 2H), 7.58 (d, *J*= 8.4 Hz, H7, 4H), 7.60-7.50 (m, H17, 1H), 7.48 (t, *J*= 7.4 Hz, H16, 2H), 7.29-7.26 (m, H12 and H10, 4H), 7.19 (d, *J*= 8.4 Hz, H6, 4H), 7.12 (d, *J*= 8.8 Hz, H2, 2H), 7.09 (dd, *J*= 5.0 and 3.8 Hz, H11, 2H); ¹³C NMR (100 MHz, CDCl₃): 195.3 (C13), 151.5 (C1), 145.8 (C5), 143.9 (C9), 138.6 (C14), 132.2 (C3), 132.0 (C17), 131.0 (C8), 130.7 (C4), 129.9 (C15), 128.4 (C11), 128.3 (C16), 127.3 (C7), 126.1 (C6), 124.9, 123.1 (C12, C10), 120.8 (C2)

Figure 3. Numbering scheme for carbon atoms in compound **2a**.



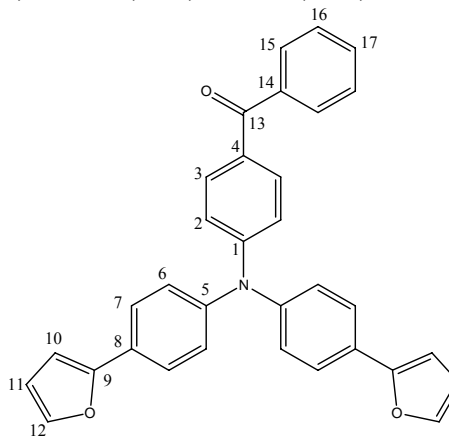
Spectroscopic data for **2b** (Figure 4): ^1H NMR (400 MHz, CDCl_3): 8.08 (d, $J=9.3$ Hz, H3, 2H), 7.61 (d, 8.6 Hz, H7, 4H), 7.30 (m, H10 and H12, 4H), 7.19 (d, $J=7.6$ Hz, H6, 4H), 7.10 (dd, $J=5.0$ and 3.6 Hz, H11, 2H), 7.04 (d, $J=9.3$ Hz, H2, 2H); ^{13}C NMR (100 MHz, CDCl_3): 152.1 (C1), 144.9 (C5), 143.5 (C9), 140.9 (C4), 132.0 (C8), 128.4 (C11), 127.5 (C7), 126.7 (C6), 125.7 (C3), 125.3 (C10 or 12), 123.5 (C10 or 12), 119.3 (C2)

Figure 4. Numbering scheme for carbon atoms in compound **2b**.



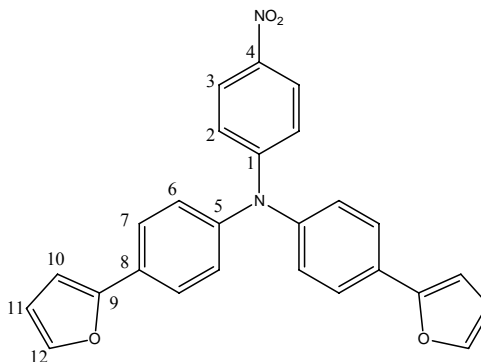
Spectroscopic data for **3a** (Figure 5): ^1H NMR (400 MHz, CDCl_3) δ 7.79 (d, $J=7.4$ Hz, H15, 2H), 7.74 (d, $J=8.6$ Hz, H3, 2H), 7.63 (d, $J=8.6$ Hz, H7, 4H), 7.55 (t, $J=7.4$, H17, 1H), 7.47 (t, $J=7.4$ Hz, H16, 2H), 7.46 (d, 1.7 Hz, H12, 2H), 7.19 (d, $J=8.6$ Hz, H6, 4H), 7.10 (d, $J=8.6$ Hz, H2, 2H), 6.61 (d, $J=3.3$ Hz, H10, 2H), 6.48 (dd, $J=3.3$ Hz and 1.7 Hz, H11, 2H); ^{13}C NMR (100 MHz, CDCl_3) δ 195.4 (C13), 153.8 (C9), 151.6 (C1), 145.7 (C5), 142.3 (C12), 138.6 (C14), 132.2 (C3), 132.0 (C17), 130.6 (C4), 129.9 (C15), 128.4 (C16), 127.5 (C8), 126.0 (C6), 125.3 (C7), 120.7 (C2), 111.9 (C11), 105.0 (C10).

Figure 5. Numbering scheme for carbon atoms in compound **3a**.



Spectroscopic data for **3b** (Figure 6): ^1H NMR (400MHz, CDCl_3): 8.07 (d, $J=9.3$ Hz, H3, 2H), 7.66 (d, 8.7 Hz, H7, 4H), 7.48 (m, $J=1.8$ Hz, H12, 2H), 7.19 (d, $J=8.7$ Hz, H6, 4H), 7.02 (d, $J=9.3$, H2, 2H), 6.65 (d, $J=3.3$ Hz, H10, 2H), 6.49 (dd, $J=1.8$ and 3.3 Hz, H11, 2H); ^{13}C NMR (100MHz, CDCl_3): 153.4 (C9), 153.2 (C1), 144.7 (C5), 142.5 (C12), 140.9 (C4), 128.5 (C8), 126.6 (C6), 125.7 (C3), 125.5 (C7), 119.3 (C2), 112.0 (C11), 105.5 (C10)

Figure 6. Numbering scheme for carbon atoms in compound **3b**.



X-ray Crystal Structures of N,N'-bis(4-(2-furanyl)phenyl)-N''-(4-nitrophenyl)amine (3b): Single-crystal X-ray diffraction data on both compounds were collected at 103°K using MoK α radiation and a Bruker APEX2 CCD area detector. Corrections were applied for Lorentz, polarization, and absorption effects. The structures were solved by direct methods and refined by full-matrix least squares on F^2 values using the programs found in the SHELXTL suite (Bruker, SHELXTL v6.10, 2000, Bruker AXS Inc., Madison, WI). Parameters refined included atomic coordinates and anisotropic thermal parameters for all non-hydrogen atoms. Hydrogen atoms on carbons were included using a riding model [coordinate shifts of C applied to H atoms] with C-H distance set at 0.96 Å. Atomic coordinates for compounds **X** and **3b** have been deposited with the Cambridge Crystallographic Data Centre.

A 0.53 x 0.18 x 0.10 mm³ crystal of **3b** was prepared for data collection coating with high viscosity microscope oil (Paratone-N, Hampton Research). The oil-coated crystal was mounted on a glass rod and transferred immediately to the cold stream (-170 °C) on the diffractometer. The crystal was triclinic in space group $P-1$ with unit cell dimensions $a = 13.9564(6)$ Å, $b = 15.1172(6)$ Å, $c = 23.1004(9)$ Å, $\alpha = 87.050(1)^\circ$, $\beta = 89.978(1)^\circ$, and $\gamma = 76.656(1)^\circ$. Data were 99.2% complete to $25.35^\circ \theta$ (approximately 0.83 Å) with an average redundancy of 2.3. The asymmetric unit contains four molecules plus two molecules of cyclohexane. POLYMORPH: The crystal was monoclinic in space group $C 2/c$ with unit cell dimensions $a = 29.111(4)$ Å, $b = 7.0385(6)$ Å, $c = 23.021(4)$ Å, $\beta = 91.410(5)^\circ$. The asymmetric unit contains a single molecule. Both furan rings are disordered over two positions. There appears to be unresolved twinning such that significant errors are still present in the model.

Calculations

All calculations were performed with the Gaussian03 program using the b3lyp DFT function. Geometries were optimized using the 6-31g(d,p) basis set.

Polymer Electrodes

In a nitrogen-purged glove box, carbon paper or platinum mesh electrodes were immersed in 0.1 M solutions of the monomer in acetonitrile that was 0.1 M in [Bu₄N]BF₄. The polymers were deposited galvanostatically with an oxidizing current

density of about 10 mA/cm² or via cyclic voltammetry with scans between 0 and 1 V vs Ag/Ag⁺ at 50 mV/sec. Subsequently, the polymer films were washed with clean acetonitrile and allowed to dry under nitrogen. The films were investigated electrochemically with cyclic voltammetry with 1 M [Bu₄N]BF₄ acetonitrile solutions, a platinum counter electrode and a Ag/Ag⁺ reference electrode. Two electrode cells composed of two polymer-coated electrodes were used to construct the polymer supercapacitors. Each capacitor was charged with a 3.5-4.5 V potential for 300 s and allowed to discharge at a set current (20 mA, 10 mV, 5 mA, and 1 mA). The resulting potential was measured over the initial 10 s of the discharge. All electrochemical measurements were performed with a PAR 273A potentiostat/galvanostat. The reported discharge potentials are not corrected for uncompensated or solution resistance.

Results and Accomplishments

Monomer Synthesis

The necessary monomers for polymerization were prepared in an efficient three-step process starting from triphenylamine as outlined in Scheme 1. The diethylaluminum chloride is the Lewis acid of choice when doing the electrophilic aromatic substitution on triphenylamine derivatives.¹⁵ Although, several cross-coupling reaction methodologies would likely work. The Stille reaction¹⁶ using the commercially available 2-(tributylstannyl)thiophene and furans is most convenient and affords the desired coupled products in excellent yields.

Monomers **2** and **3** were characterized by detailed NMR spectroscopic analysis with complete assignments in the proton and carbon spectra. In selected cases we have performed single-crystal x-ray analyses to obtain exact solid-state structural information for use in conjunction with molecular orbital calculations. The molecular structures as determined by single-crystal x-ray diffraction for the monomer **3b** (Figure 6) reveal the expected triaryl moieties binding to a centralized nitrogen. Furthermore, the substitution of the aryls at the 4 position is confirmed. A summary of the crystallographic data collection parameters is presented in Table 1.

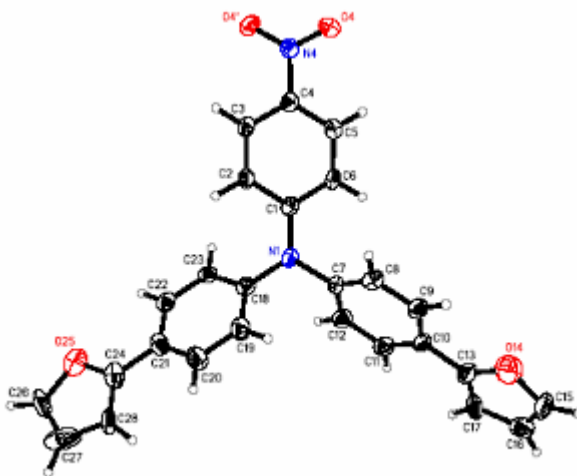


Figure 6. Structure of **3b**.

Table 1. Crystal data and structure refinement for **3b**.

Empirical formula	C ₅₈ H ₄₈ N ₄ O ₈	
Formula weight	929.00	
Temperature	103(1)°K	
Wavelength	0.71073 Å	
Crystal system	Triclinic	
Space group	P -1	
Unit cell dimensions	a = 13.9564(6) Å	α = 87.050(1)°
	b = 15.1172(6) Å	β = 89.978(1)°
	c = 23.1004(9) Å	γ = 76.656(1)°
Volume	4735.6(3) Å ³	
Z	4	
Density (calculated)	1.303 Mg/m ³	
Absorption coefficient	0.087 mm ⁻¹	
F(000)	1952	
Crystal size	0.53 x 0.18 x 0.10 mm ³	
Theta range for data collection	0.88 to 25.35°	
Index ranges	-16 ≤ h ≤ 13, -18 ≤ k ≤ 18, -27 ≤ l ≤ 27	
Reflections collected	40296	
Independent reflections	17217 [R(int) = 0.0421]	
Completeness to θ = 25.35°	99.2 %	
Absorption correction	Semi-empirical from equivalents	
Max. and min. transmission	0.9910 and 0.9550	
Refinement method	Full-matrix least-squares on F ²	
Data / restraints / parameters	17217 / 0 / 1261	
Goodness-of-fit on F ²	0.996	
Final R indices [I > 2σ(I)]	R1 = 0.0621, wR2 = 0.1928	
R indices (all data)	R1 = 0.1594, wR2 = 0.2526	
Largest diff. peak and hole	0.571 and -0.465 e.Å ⁻³	

The new compounds **2** and **3** contain two different reactive centers: the triaryl ammine and furanyl or thiophenyl groups. The triaryl ammine group has a well-known redox activity which can be chemically tuned by judicious choice of substituents on the aromatic rings. For example, each additional chlorine anodically shifts the oxidation potential approximately 250 mV. The synthesis of the new compounds is easily modified to accommodate other ring substituting reactions in addition to the acylation and nitration process. The nitro and benzoyl derivatives demonstrate the versatility of the synthetic process. The triaryl ammine groups are capable of undergoing electrochemical and redox activated polymerization. However, this process is extremely slow and proved ill-suited to generating polymer films. To facilitate polymerization, the two furanyl and thiophenyl groups were added to the aromatic rings. Both of these five-membered rings are known to undergo electrochemical polymerization upon oxidation at potentials in excess of 2 V vs SCE. Furthermore, the furanyl and thiophenyl groups will also shift the oxidation potential of the ammine. Using our approach electron-donating or electron-withdrawing groups can be added so as to rationally shift the oxidation potential in a specific direction.

In order for the furanyl and thiophenyl groups to act as cross-linking units, the highest-occupied molecular orbital (HOMO) must have some electron density located on the five-membered rings. Thus, when an electron is removed from this orbital, the free radical on the cation will be partially located on these units and initiate polymerization. The crystal structure of **3b** allows for density function theory to calculate the electron distribution in the molecule. Figure 7 reveals the HOMO of **3b** and the radical cation **3b**⁺. Importantly, the HOMO of **3b**⁺ contains electron density in the vicinity of the furanyl rings. The presence of the free radical on the five-membered rings, activates the furanyl groups to polymerize forming difuranes.

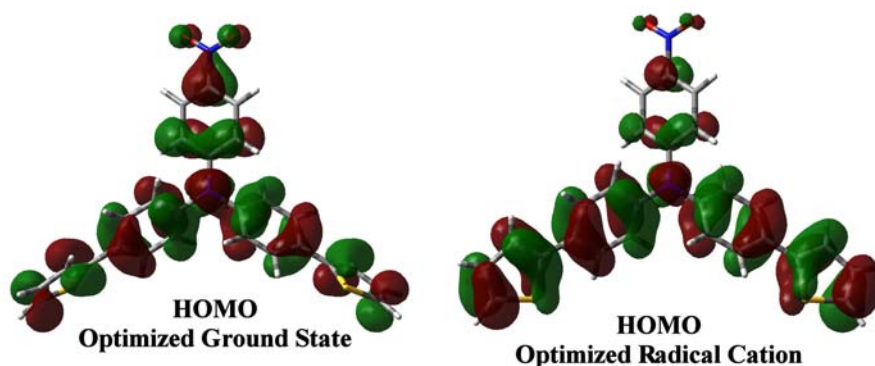


Figure 7. HOMO of **3b** (left) and the first cation of **3b** (right).

Polymer films

The new monomers undergo electrochemical polymerization at relatively low oxidation potentials of 1 V or less vs. Ag/Ag⁺, Figure 8. In the oxidized form, triphenyl ammonium undergoes a very slow polymerization process,¹⁷ and free thiophenes and furans require relatively high potentials in excess of 2 V for facile polymerization. In the present case, the triaryl ammine functionality of **2** and **3** is oxidized at the low potential

and the generated radical, which is partially located on the furanyl and thiophenyl groups, facilitates the polymerization of the five-membered rings. Thus, the furan and thiophene groups of **2** and **3** are crosslinked (polymerized) at potentials considerably lower than that needed to polymerize free furan and thiophene, Figure 8.

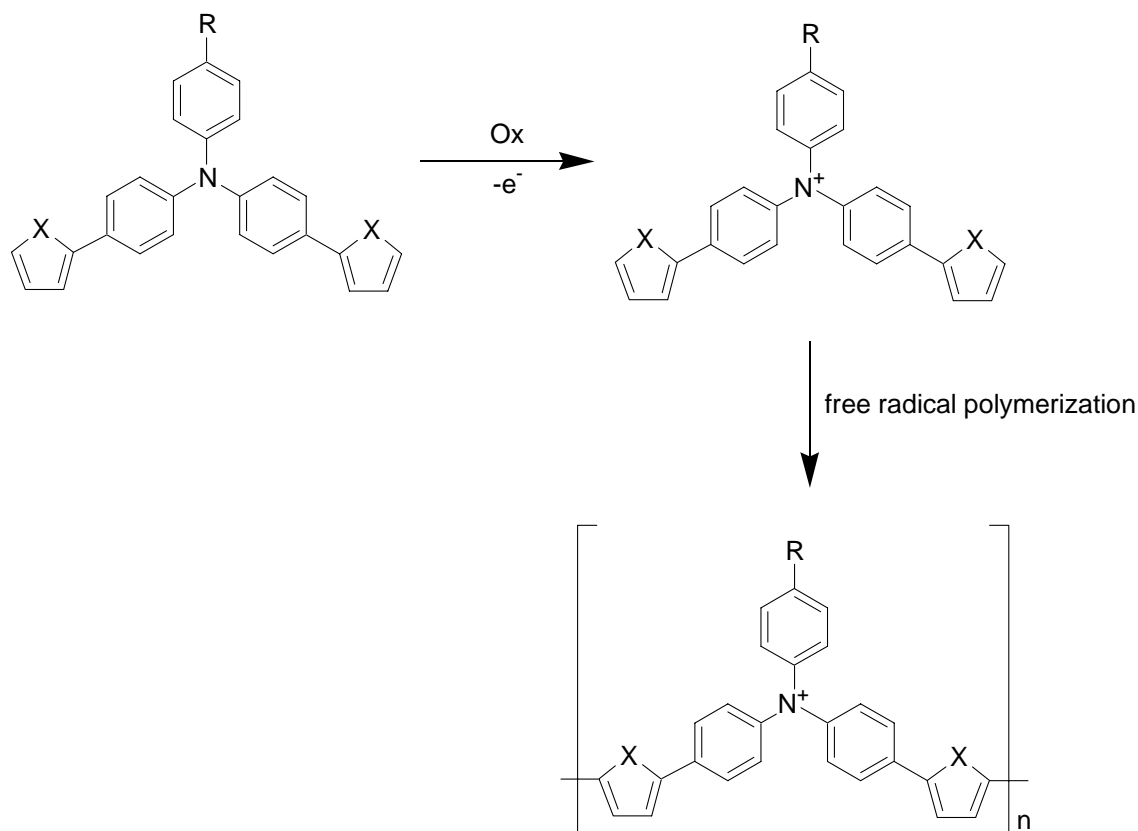


Figure 8. Stepwise polymerization of **2** and **3** occurs via the initial oxidation of the ammine. The cation radical is delocalized about the five-membered rings allowing the furanyl and thiophenyl rings to undergo polymerization.

Polymer films of **2** and **3** could be grown via cyclic voltammetry or by galvanostatic methods, Figure 9. However, excessive deposition times results in thick polymers layers that were not electrochemically active. Electrochemical polymerization of monomers occurs at approximately 0.6 V vs Ag/Ag⁺. Cycling the potential of a platinum electrode in a solution of the monomer results in increasing current with each subsequent sweep. This increase is a result of the formation of the parent polymer as a film on the working electrode, Figure 4. Alternatively, polymer films can be grown galvanostatically with anodic currents. For the present work, this technique was preferred because it allowed the polymer thickness of the films to be more precisely controlled.

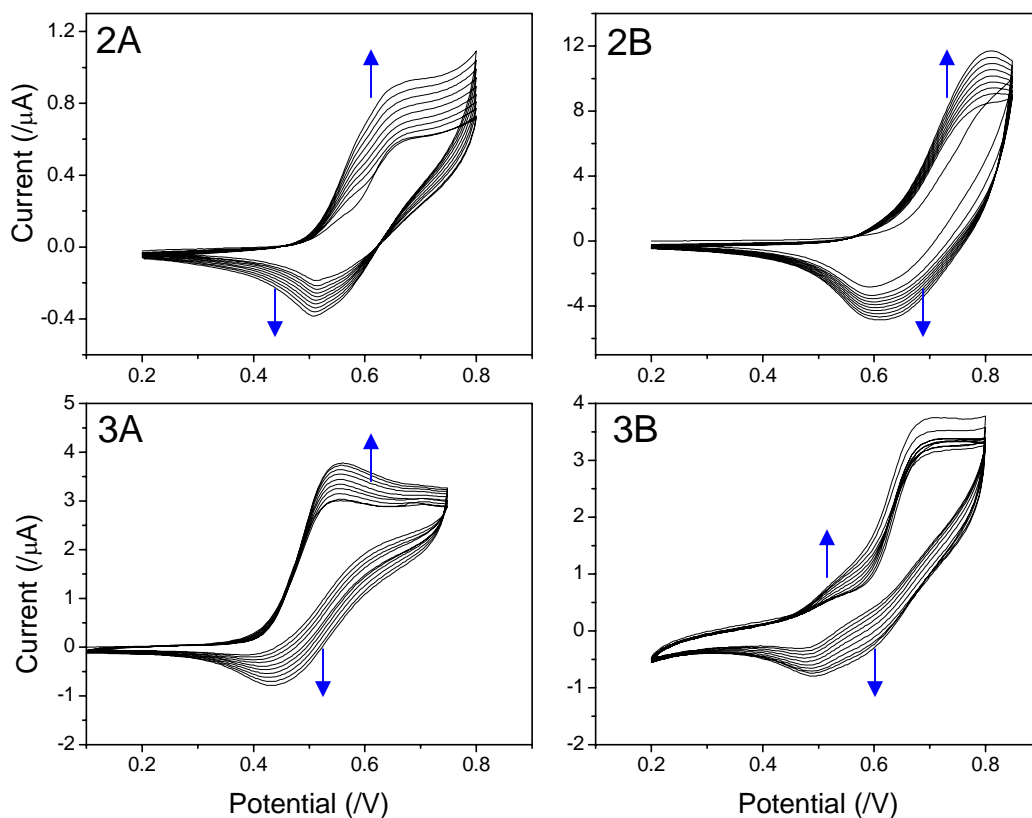


Figure 9. Cyclic voltammograms of **2** and **3** at Pt electrodes in 0.1 M solution of monomer in acetonitrile with 0.1 M [Bu₄N]BF₄ electrolyte. Potentials are vs Ag/Ag⁺. With each subsequent sweep additional polymer is deposited on the electrode as evident by the increasing currents.

The electrochemical doping of each polymer derived from **2** and **3** is dependent on the monomer type. Cyclic voltammetry on the polymer films in clean electrolytes reveals both the oxidative and reductive potentials of the film, Figure 10. In assembling a supercapacitor from two polymers, the upper limit of the output voltage is determined by the difference in the reduction potential of the n-type polymer and the oxidation potential of the *p*-type polymer. The new polymers were designed to exhibit more positive oxidation potentials than the polythiophenes used in the first year of this SERDP program (approximately 0.6 V). In this capacity, the new polymers are anticipated to serve as cathodes (*p*-type) polymers. By employing polymers with larger oxidation potentials, the total energy output of the polymer supercapacitors can be significantly increased. Under the first year of effort, suitable energy and power outputs were already demonstrated using the lower voltage material. This new effort is aimed at improving on the performance of the improved cathode materials.

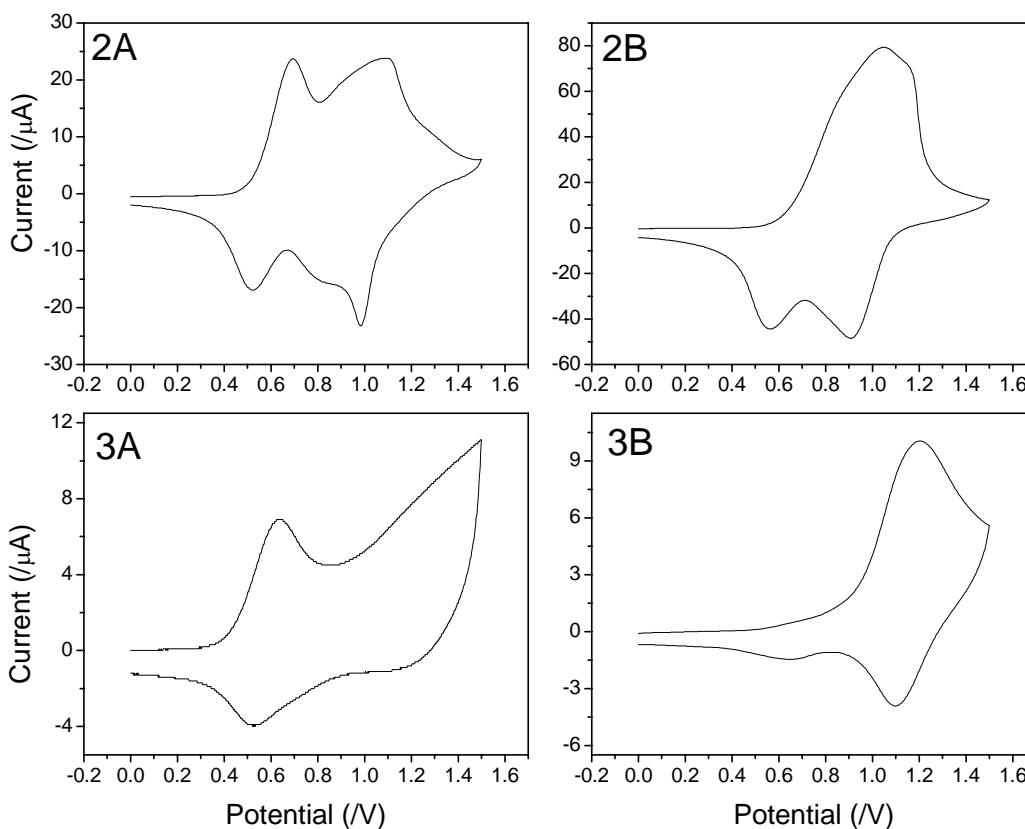


Figure 10. Cyclic voltammograms of **2** and **3** on platinum disk electrodes with 0.1 M $[\text{Bu}_4\text{N}]\text{BF}_4$ in CH_3CN electrolyte. Potentials are vs Ag/Ag^+ .

Polymers derived from **2** and **3b** undergo multiple oxidation steps. The first process (0.4-0.7 V) is associated with the oxidation of the ammine functionality. Clearly, this potential is most sensitive to the presence of the nitro and benzoyl groups. The benzoyl group is less electron-withdrawing than nitro and the furan with the more electronegative oxygen is more electron-withdrawing than the thiophene. The second oxidation waves observed for **2** and **3b** is likely due to the oxidation of the bifurane or bithiophene groups. Alternatively, the second oxidation wave may be due to removing an electron from the same molecular orbitals that the first electron is removed. Since this second electron is removed from a cationic species, its oxidation potential is shifted positive. *These results demonstrate that the oxidation potentials of these new polymers can be rationally controlled by synthesizing monomers with specific electronic properties.* Furthermore, with slight variations on the substituents on the aryl ammine group, we can significantly alter the electrochemical potential of the polymers in a specific direction.

Most important is the combined effect of the nitro and furan groups on the oxidation potential of the polymer derived from **3b**. The furan and nitro moieties are sufficient to shift the oxidation of **3b** above 1 V vs Ag/Ag⁺. This anodic potential is 0.3-0.5 V more positive than the polythiophenes studied previously under this SERDP project. Supercapacitors employing polymers derived from **3b** as cathode materials are expected to have significant increases in thermodynamic performance. Future generations of these materials can make use of the additional substitution sites available to further tune the electronic properties of the polymer.

Polymer Supercapacitors

The discharge properties of the polymer supercapacitors are a function of the types of polymers used in the anode and cathode, electrolyte, charging time, charging potential, and temperature. These variables were explored previously under this SERDP program. Our current focus is to investigate the performance of supercapacitors fabricated from the new polymers with high oxidation potentials. For this aspect of the program we employed polymers derived from **3b** as this was the only new polymer to demonstrate significantly higher oxidation potentials. Electrochemical charging of the polymer supercapacitors is accomplished by biasing one polymer electrode verses the other in a two-electrode configuration. The direction of the bias determines which film is oxidized (*p*-doped) or reduced (*n*-doped). In the present work, polymer supercapacitors were charged at 4 V for approximately 300 s. The charging current rapidly decreases over the first two minutes and eventually plateaus. The fabrication, charging, and discharging experiments are similar to those reported under SERDP PP-1359 previously. In the present work, polymer cathodes derived from **3b** were used in combination with polythiophene and poly(3-methylthiophene) anodes.

In the present work, acetonitrile electrolytes with 0.1 M [Bu₄N]BF₄ were employed for all measurements. Previous work on this project demonstrated that the tetrabutylammonium cation is not ideally suited for supercapacitor performance. Replacing tetrabutylammonium with the smaller tetramethylammonium cation significantly increases the discharge properties of the polythiophene devices. The choice

of tetrabutylammonium or tetramethylammonium electrolytes is expected to only affect the performance of the anode rather than the cathode, which the new polymers are expected to improve. In this case the cathode discharging is dependent on the anion BF_4^- . Currently, we are primarily focused on understanding the differences and possible advantages of the new polymer cathodes compared to the polythiophene devices rather than designing and tuning the devices for optimal performance. Thus, supercapacitors using the $[\text{Bu}_4\text{N}]\text{BF}_4$ electrolyte are equally well suited for comparing the different polymers and their discharge properties.

The discharge potentials of the charge capacitors were monitored during the initial ten seconds at various constant discharge currents of 1 mA, 5 mA, 10 mA, and 20 mA, Figure 11. Compared to the devices that surpassed SERDP's requirements under these less optimal conditions, *the new polymers proved superior to the polythiophenes that provide the required 20 mA at 2 V. The energy output of the new polymer supercapacitor is 20 % greater than that previously reported.* Although, the performance of these current devices does not meet the required metrics set by SERDP (20 mA at 2 V for two devices in series), the new cathode material outperforms both the polythiophene and poly(3-methylthiophene) cathodes studied previously. Thus, we have demonstrated that the novel polymers with a tunable oxidation potential can provide cathode materials with superior performance to the conventional polythiophenes under similar conditions.

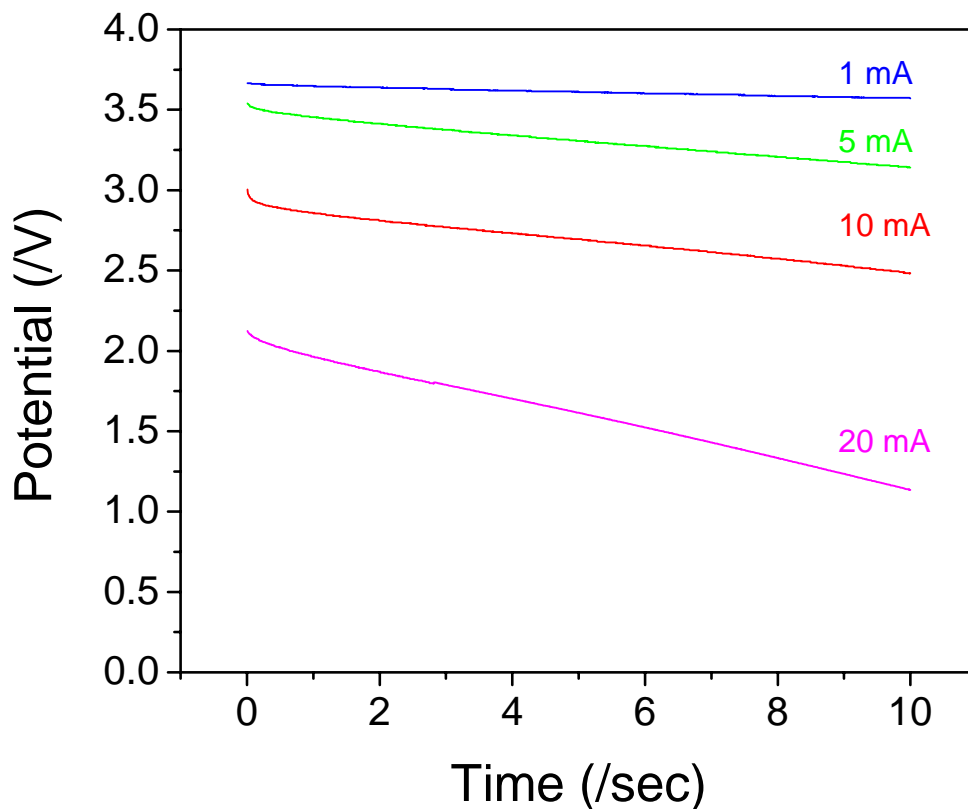


Figure 11. Discharge potentials for polymer supercapacitors composed of (A) polythiophene (anode) and poly-**3b** (cathode) with 0.1 M $[\text{Bu}_4\text{N}]\text{BF}_4$ in CH_3CN electrolytes.

Conclusions

Novel polymers with tunable redox centers were synthesized from bisfuranyl-triarylammine and bithiophenyl-triarylammine monomers. The oxidation potential of the ammine functionality is highly dependent on the substituents on the aryl rings with a total variation of 0.3 V between the four new compounds reported. Oxidation of the triarylammine results in a cross linking of the furanyl or thiophenyl groups and the formation of a polymer film. Consequently, the new polymers can be generated electrochemically at potentials that are considerably less positive than that needed to polymerized conventional polythiophenes and polyfurans.

The oxidation potentials of these new polymers are similarly dependent on the nature of the substituents on the aryls. The four new polymers generated by **2** and **3** display oxidation potentials that span approximately 0.6 V. Thus, by judicious choice of substitution, one can engineer the redox properties of the monomer and subsequent polymer. This strategy provides a straightforward route to designing polymer materials with specific and tailorable electronic properties. Polymers derived from **3b** which contain the electron-withdrawing furan and nitro groups are electrochemically oxidized at 1.1 V vs Ag/Ag⁺, 0.5 V more positive than conventional polythiophenes.

*Supercapacitors constructed from **3b**, the best performing (highest oxidation potential) of the new polymers, provide 20 % more energy than the best performing polythiophene supercapacitors with [Bu₄N]BF₄ electrolytes that were reported previously.*

References

- (1) Besenhard, J.O., Ed. *Handbook of Battery Materials*, Wiley-VCH, Weinheim, 1999.
- (2) Pistoia, G. Ed. *Lithium Batteries New Materials, Developments and Perspectives*, Elsevier, Amsterdam, 1994
- (3) Vincent, C.A.; Scrosati, B. *Modern Batteries*, John Wiley & Sons Inc., New York, 1997.
- (4) Novák, P.; Müller, K.; Santhanam, K.S.V.; Haas, O. *Chem. Rev.* **1997**, *97*, 207-281.
- (5) Stenger-Smith, J.D. *Prog. Polym. Sci.* **1998**, *23*, 57-79.
- (6) Laforgue, A.; Simon, P.; Sarrazin, C.; Fauvarque, J.-F. *J. Power Sources* **1999**, *80*, 142-148.
- (7) Yoon, C.O.; Moses, D.; Heeger, A.J.; Cao, Y.; Chen, T.-A.; Wu, X.; Rieke, R.D. *Synth. Met.* **1995**, *75*, 229-239.
- (8) Bruckenstein, S.; Wilde, C.P.; Shay, M.; Hillman, A.R.; Loveday, D.C. *J. Electroanal. Chem.* **1989**, *258*, 457-462.
- (9) Heeger, A.J. *J. Phys. Chem. B* **2001**, *105*, 8475-8491.
- (10) MacDiarmid, A.G. *Angew. Chem. Int. Ed.* **2001**, *40*, 2581-2590.
- (11) Ghosh, S.; Inganas, O. *Electrochem. Solid State Lett.* **2000**, *3*, 213-215.
- (12) Marque, P.; Roncali, J.; Garnier, F. *J. Electroanal. Chem.* **1987**, *107*, 107-118.
- (13) Ratner, M.A.; Shriver, D.F. *Chem. Rev.* **1988**, *88*, 109-124.
- (14) Wei, X.Y.; Shriver, D.F. *Chem. Mater.* **1998**, *10*, 2307.
- (15) Wright, M. E.; Jin, M.-J. *J. Org. Chem.* **1989**, *54*, 965.
- (16) Stille, J. K. *Angew. Chem. Int. Ed. Engl.* **1986**, *25*, 508. For a more general review on cross-coupling reactions to make aryl-aryl bonds see: Hassan, J.; Sevignon, M.; Gozzi, C.; Schulz, E.; Lemaire, M. *Chem. Rev.* **2002**, *102*, 1359-1469 and references cited therein.
- (17) Connelly, N.G.; Geiger, W.E. *Chem. Rev.* **1996**, *96*, 877.